Journal of Crystal Growth 310 (2008) 3084–3092

Contents lists available at ScienceDirect

Journal of Crystal Growth

journal homepage: www.elsevier.com/locate/jcrysgro

Equilibrium strain-energy analysis of coherently strained core–shell nanowires

Thomas E. Trammell, Xi Zhang, Yulan Li, Long-Qing Chen, Elizabeth C. Dickey *

Department of Materials Science and Engineering, Materials Research Institute, The Pennsylvania State University, University Park, PA 16802, USA

ARTICLE INFO

Article history:
Received 8 November 2007
Received in revised form
5 February 2008
Accepted 26 February 2008
Communicated by R.M. Biefeld
Available online 8 March 2008

PACS:
61.46.Km
61.72.uf
62.20.D

Keywords:
A1. Stresses
A3. Solid phase epitaxial
B2. Semiconductor materials
B3. Field effect transistors

ABSTRACT

In order to continue the performance enhancement of Si-based semiconductor devices, the number of devices on a chip as well as the performance of those devices must continue to improve. One method for improving device functionality is the incorporation of strained Si–Ge heterostructures. While such heterostructures have been the focus of much research in planar Si processing, only recently has the fabrication of such heterostructures in nanoscale semiconductors been addressed. In particular, the fabrication of a Si–Ge radial nanowire heterostructure requires a consideration of the epitaxial stability of the shell on the underlying core nanowire. This work develops a model for the strain state of a radial nanowire heterostructure, focusing on the particular example of Si–Ge. The behavior of the radial nanowire heterostructure is compared to that of a planar heterostructure, and we find that much higher strains can be achieved in the nanowire geometry.

1. Introduction

The reliable and controlled fabrication of semiconductor heterostructures has for decades made possible the development of many new devices as well as improvements in speed in existing devices [1]. More recently, the ability to synthesize semiconductor nanowires has opened the door for many novel devices in which the advantages of heterostructures can be incorporated into nanoscale devices. It has been shown that axial heterostructure nanowires can be grown, in which the composition of the nanowire is changed during growth [2–4]. Such devices have great potential in optical and electronic applications in which quantum confinement leads to behavior differing from the bulk. In addition to axial heterostructures, radial heterostructures hold great promise for many unique devices, such as nanowire FETs and nanoscale optical cavities [4]. Several groups have devised methods of making these radial core–shell heterostructures [3–6], but the exact limitations on epitaxial growth have not been fully explored.

One critical feature of these nanoscale heterostructures is the quality of the interface. As is true for conventional planar heterostructures, it is desirable to produce epitaxial, or fully coherent, layers without interfacial defects. Much work has been done on epitaxial thin films grown on planar substrates to determine conditions for epitaxial growth without defects [7,8]. The two layers will, in general, have different lattice parameters, thus introducing a coherency strain in an epitaxial system. In planar films, the strain energy can be relieved by bending (in the case of thin substrates) [9], by the introduction of misfit dislocations at the interface [8], or by a transition from 2D film growth to 3D island growth (i.e. Stranski–Krastanow growth) [10,11]. In systems in which bending is not possible, there exists a critical film thickness above which perfect 2D epitaxy fails, and any devices using such a heterostructure may lose functionality [7]. If one uses thin enough substrates, however, this critical thickness can be increased by allowing the substrate and the film to partition the strain energy [12,13].

Epitaxial lattice-mismatched structures also provide an opportunity to control the strain state of the system. Tensile-strained silicon grown on a Si_xGe_{1-x} layer has been shown to exhibit a sizeable electron mobility increase relative to bulk Si [14,15], and compressively strained Si_xGe_{1-x} structures grown on a Si substrate have been shown to exhibit a higher hole mobility relative to bulk [16,17]. Similarly in nanowires, by judicious selection of the core and shell compositions as well as the thickness, it may be possible to engineer the strain state of a nanowire to achieve similar mobility increases.

* Corresponding author. Tel./fax: +1 814 865 9067.
E-mail address: ecd10@psu.edu (E.C. Dickey).

0022-0248/$ - see front matter © 2008 Elsevier B.V. All rights reserved.
doi:10.1016/j.jcrysgro.2008.02.037

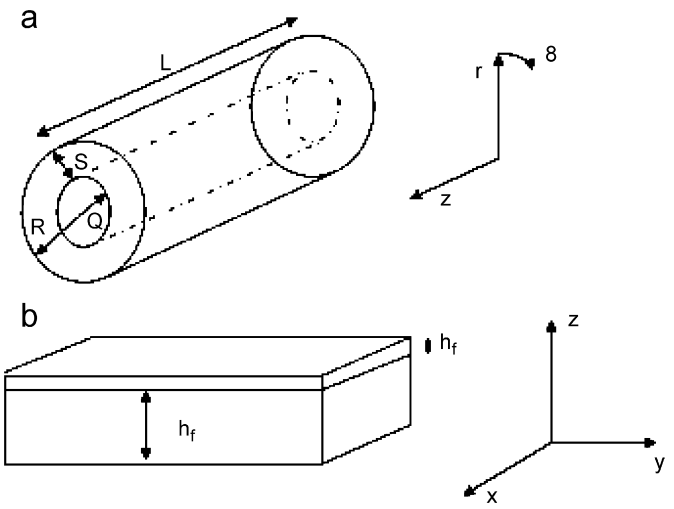

Fig. 1. Schematic of a (a) core–shell structure and a (b) thin film, substrate structure with coordinate axes defined.

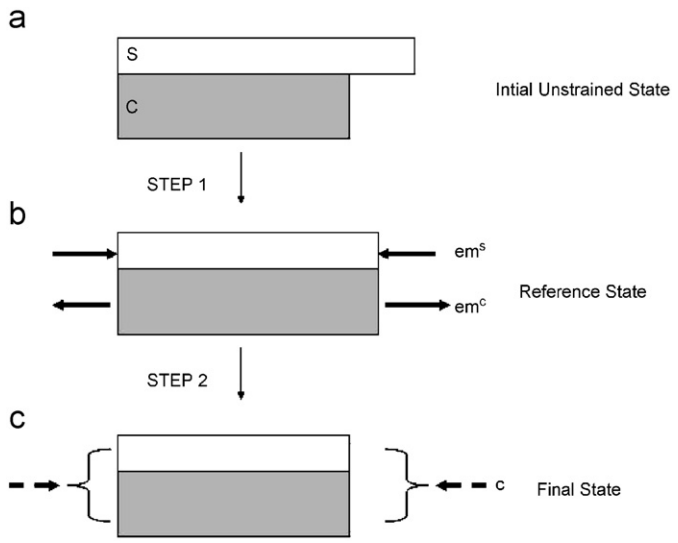

Fig. 2. Representation of a two-step process from (a) the initial state to (b) the reference state and finally to (c) the final epitaxial state.

The purpose of this paper is to develop an elasticity model for studying the behavior of core–shell nanowires and to compare the results with the known behavior of the planar system. The distinct geometries of the two systems (see Fig. 1) lead to profound differences in the limitations and behavior of epitaxy in the two systems. Based on the previous work on Si–Si_xGe_{1-x} planar systems, particular attention will be paid to the Si–Si_xGe_{1-x} core–shell nanowire system.

2. The model

The development of the elasticity model closely follows the work by Warwick and Clyne [18] in their consideration of the mismatch in thermal expansion in concentric fibers. We ignore facets at the interface assuming the interface is cylindrical, thus allowing the development of the model in cylindrical coordinates. It is recognized, however, that in actual nanowires faceting can occur and more complex models would need to be developed to understand the role of this faceting.

This section develops the model used to determine the strain state of the system. After the model has been described mathematically, it is utilized to solve analytically for the strain state of the core–shell system (for definitions of the dimensions used, Q, R, S, L, refer to Fig. 1a). As a note on the mathematical symbols used, a superscript denotes the layer (c for core and s for shell), and a subscript denotes either the direction (i.e., r, θ, z) or the fact that it is an initial state (the subscript o is used).

The model considers a system in which the two layers are cubic in their unstrained states, with lattice parameters of a_o^c and a_o^s. In the initial state, the core and shell lattices are incoherent and there is no strain in either layer. In order to determine the final strain state of the coherent system, a two-step process of equilibration is modeled. Fig. 2 is a simplified depiction of these two steps in a planar arrangement. The first step is the establishment of coherent epitaxy, as shown in Fig. 2b. This step puts the system in an arbitrary reference state to which both layers are coherently strained to the same lattice parameter. This reference state is mathematically represented by the lattice spacing of a reference, a_o^r. The choice of reference state does not affect the final solution. Thus, the lattice spacings of the core and the shell are all initially strained to a_o^r to establish a coherent epitaxial arrangement. The associated misfit strain, em_o^n, is defined as the strain between the initial state and the reference state such that

$$em_o^n = \frac{a_o^n - a_o^r}{a_o^r} \tag{1}$$

The above equation can easily be modified to produce a misfit strain that is dependent on direction if one wishes to consider a non-cubic system or different reference states in each direction. For the example of Si and Ge, however, cubic symmetry is maintained in the unstrained state as well as in the reference state.

Now that the entire system is strained to the reference state, the second step is that the system is allowed to elastically relax to the final state, as shown in Fig. 2b. Displacements from the reference state are defined in all three directions in each layer, u_i^n. In order to maintain the epitaxy provided by step one, the displacements at the interface must be continuous at the interface. In other words, at $r = Q$

$$u_z^c = u_z^s \tag{2a}$$

$$u_\theta^c = u_\theta^s \tag{2b}$$

$$u_r^c = u_r^s \tag{2c}$$

These displacements lead to what is termed "displacement strains" on the system, denoted by ε_i^n. The displacement strains (again in terms of the reference layer) are expressed as

$$\varepsilon_i^n = \frac{a_i^n - a_o^r}{a_o^r} \tag{3}$$

In (3), a_i^n represents the lattice spacing after the system has relaxed to its final state.

The displacement strains, ε_{ij}^n, are related to the displacement functions, u_i^n, as follows [19]:

$$\varepsilon_{rr}^n = \frac{\partial(u_r^n)}{\partial r} \tag{4a}$$

$$\varepsilon_{\theta\theta}^n = \frac{1}{r}\frac{\partial(u_\theta^n)}{\partial\theta} + \frac{u_r^n}{r} \tag{4b}$$

$$\varepsilon_{zz}^n = \frac{\partial(u_z^n)}{\partial z} \tag{4c}$$

$$\varepsilon_{\theta z}^n = \frac{1}{2}\left(\frac{\partial(u_z^n)}{\partial r} + \frac{\partial(u_r^n)}{\partial z}\right) \tag{4d}$$

$$\varepsilon^n_{\theta z} = \frac{1}{2}\left(\frac{\partial(u^n_\theta)}{\partial z} + \frac{1}{r}\frac{\partial(u^n_z)}{\partial \theta}\right) \tag{4e}$$

$$\varepsilon^n_{r\theta} = \frac{1}{2}\left(\frac{1}{r}\frac{\partial(u^n_r)}{\partial \theta} + \frac{\partial(u^n_\theta)}{\partial r} - \frac{u^n_\theta}{r}\right) \tag{4f}$$

Assuming that the system exhibits radial symmetry, several simplifications are made. First, there is no displacement in the tangential direction:

$$u^n_\theta = 0 \tag{5a}$$

Also, as a consequence of the cylindrical symmetry,

$$u^n_r = u^n_r(r) \tag{5b}$$

$$u^n_z = u^n_z(z) \tag{5c}$$

Inserting Eq. (5a–c) into Eq. (4a–f) and simplifying the notation, we obtain

$$\varepsilon^n_{rr} = \frac{\partial(u^n_r)}{\partial r} = \varepsilon^n_r \tag{6a}$$

$$\varepsilon^n_{\theta\theta} = \frac{u^n_r}{r} = \varepsilon^n_\theta \tag{6b}$$

$$\varepsilon^n_{zz} = \frac{\partial(u^n_r)}{\partial z} = \varepsilon^n_z \tag{6c}$$

$$\varepsilon^n_{rz} = \varepsilon^n_{\theta z} = \varepsilon^n_{r\theta} = 0 \tag{6d}$$

After both the misfit compensation (step 1) and the elastic relaxation (step 2), the total elastic strain, e^n_i, is obtained. Due to the sign convention used in Eq. (1), the total elastic strain in each layer is expressed as

$$e^n_i = \frac{a^r_o}{a^n_o}(\varepsilon^n_i - em^n_o) \tag{7}$$

The leading term expressed in Eq. (7) is a correction factor that allows the elastic strain of an individual layer to be in terms of that layer rather than the reference state. This represents the strain state of each phase in the nanowire in the most general form.

The next step is to solve for general forms of the displacement functions to calculate the total strains associated with the system. The first boundary conditions applied to the system are the stress equilibrium relations in cylindrical coordinates such that there is no net force on any body element [19]:

$$\frac{1}{r}\frac{\partial(\sigma^n_r r)}{\partial r} + \frac{1}{r}\frac{\partial\tau^n_{r\theta}}{\partial\theta} + \frac{\partial\tau^n_{rz}}{\partial z} - \frac{\sigma^n_\theta}{r} = 0 \tag{8a}$$

$$\frac{1}{r}\frac{\partial\sigma^n_\theta}{\partial\theta} + \frac{\partial\tau^n_{\theta z}}{\partial z} + \frac{\partial\tau^n_{r\theta}}{\partial r} - \frac{2\tau^n_{r\theta}}{r} = 0 \tag{8b}$$

$$\frac{1}{r}\frac{\partial(\tau^n_{rz} r)}{\partial r} + \frac{1}{r}\frac{\partial\tau^n_{\theta z}}{\partial\theta} + \frac{\partial\sigma^n_z}{\partial z} = 0 \tag{8c}$$

The stresses are expressed in terms of the elastic strains multiplied by the stiffness matrix. For cubic crystal structures, the stiffness matrix simplifies to

$$\begin{bmatrix} C^n_{11} & C^n_{12} & C^n_{12} & 0 & 0 & 0 \\ C^n_{12} & C^n_{11} & C^n_{12} & 0 & 0 & 0 \\ C^n_{12} & C^n_{12} & C^n_{11} & 0 & 0 & 0 \\ 0 & 0 & 0 & C^n_{44} & 0 & 0 \\ 0 & 0 & 0 & 0 & C^n_{44} & 0 \\ 0 & 0 & 0 & 0 & 0 & C^n_{44} \end{bmatrix}$$

which results in the following simplified expressions for stress:

$$\sigma^n_r = C^n_{11}e^n_r + C^n_{12}e^n_\theta + C^n_{12}e^n_z \tag{9a}$$

$$\sigma^n_\theta = C^n_{12}e^n_r + C^n_{11}e^n_\theta + C^n_{12}e^n_z \tag{9b}$$

$$\sigma^n_z = C^n_{12}e^n_r + C^n_{12}e^n_\theta + C^n_{12}e^n_z \tag{9c}$$

$$\tau^n_{rz} = \tau^n_{\theta z} = \tau^n_{r\theta} = 0 \tag{9d}$$

This provides expressions for the stresses of the layers in terms of the displacement functions and the lattice spacings. Inserting Eq. (9a–d) into Eq. (8a–c):

$$\frac{d^2(u^n_r)}{dr^2} + \frac{1}{r}\frac{d(u^n_r)}{dr} - \frac{u^n_r}{r^2} = 0 \tag{10a}$$

$$\frac{d^2(u^n_z)}{dz^2} = 0 \tag{10b}$$

Eq. (10a,b) can be satisfied by the following displacement functions:

$$u^n_r = A^n r + \frac{B^n}{r} \tag{11a}$$

$$u^n_z = E^n z + F^n \tag{11b}$$

Now the entire strain state of the system is expressed in terms of eight unknowns (A^c, B^c, E^c, F^c, A^s, B^s, E^s and F^s). Of course, these unknowns and thus the strain state of the system depend on the relevant dimensions of the core–shell structure (Q, R, S) as well as the unstrained lattice spacings of the core, shell, and the reference state.

Other constraints on the system and how they can be used to solve for the unknowns mentioned above are now examined. Because the displacements must be continuous, there are two initial constraints on the system:

i. According to Eq. (2a) the displacement in the axial direction should be continuous.
This constraint maintains epitaxy such that $a^c_z|_{r=Q} = a^s_z|_{r=Q}$.
ii. According to Eq. (2c) the displacement in the radial direction should be continuous.
This constraint maintains epitaxy such that $a^c_\theta|_{r=Q} = a^s_\theta|_{r=Q}$.
Since there is no applied force on the system, the forces on all surfaces of the system are zero.
iii. There is no net force on the surface perpendicular to the z-direction:

$$\int_0^Q \int_0^{2\pi} \sigma^c_z r\,dr\,d\theta + \int_Q^R \int_0^{2\pi} \sigma^s_z r\,dr\,d\theta = 0 \tag{12}$$

iv. There is no net force on the surface perpendicular to the r-direction:

$$\sigma^s_r|_{r=R}| = 0 \tag{13}$$

And finally:
v. All displacements, strains, and stresses must be finite throughout the system.
Examining the equations for displacement above, we can see that in the core at $r = 0$, $u^c_r = \infty$ unless B^c is zero. Therefore,

$$B^c = 0 \tag{14}$$

vi. At the interface, the stresses in the radial direction should be continuous:

$$\sigma^c_r|_{r=Q} = \sigma^s_r|_{r=Q} \tag{15}$$

As a consequence of Eq. (2a), $F^c = F^s = 0$, and $E^s = E^c$. Thus, Eq. (2a) eliminates three unknowns, Eq. (14) eliminates another, and we are left with four unknowns (A^c, E^c, A^s, B^s) and four more constraint Equations (2c), (12), (13) and (15). Using the definitions

of stress, strain, and displacement given above, a simple matrix elimination method can be used to solve for the displacements (and thus displacement strains, elastic strains, and stresses) in terms of the dimensions of the structure, the lattice spacings of the core and the shell, the elements of the stiffness matrix, and the reference state a_0^r. Since we have already mentioned that the choice of a_0^r is arbitrary, we have set a_0^r equal to a_0^c in order to simplify some of the expressions (i.e., $em_0^c$is now zero).

While the strain state of the system is useful, we ultimately need to determine the energy associated with the strained core–shell system, so that we may examine issues of stability. The elastic strain energy of each layer is denoted by U and is calculated as follows:

$$U^c = \frac{1}{2}\int_0^L dz \int_0^Q dr \int_0^{2\pi} \sigma_i^c e_i^c r \, d\theta \tag{16a}$$

$$U^s = \frac{1}{2}\int_0^L dz \int_Q^R dr \int_0^{2\pi} \sigma_i^s e_i^s r \, d\theta \tag{16b}$$

In particular, we are concerned with the elastic strain energy per area (J/m^2) of both the shell and the core. We denote the elastic strain energy originating per interfacial area as

$$\hat{U}^c = \frac{1}{2Q}\int_0^Q \sigma_i^c e_i^c r \, dr \tag{17a}$$

$$\hat{U}^s = \frac{1}{2Q}\int_Q^R \sigma_i^s e_i^s r \, dr \tag{17b}$$

This model is general in its treatment of an arbitrary core and shell material, provided they are both cubic. Since nanowire heterostructures of Si and Ge are of great interest for their compatibility with existing integrated circuit technology, we examine how a structure with a Si core and a Ge shell behaves. The lattice constants of Si and Ge are 5.431 and 5.657 Å, respectively [20]. The stiffness tensor elements of the system at room temperature are, for Si [21]: $C_{11} = 165.8$ GPa, $C_{12} = 63.9$ GPa, $C_{44} = 79.6$ GPa; for Ge [21]: $C_{11} = 128.5$ GPa, $C_{12} = 48.3$ GPa, $C_{44} = 66.8$ GPa. While we model the ⟨100⟩ growth axis in this paper, it should be noted that the Si_xGe_{1-x} nanowire growth directions are predominantly ⟨111⟩, ⟨110⟩, and ⟨112⟩ when grown via vapor–liquid–solid techniques [22–26], although ⟨100⟩ Si nanowire arrays can be fabricated by bottom-down lithography and etching approaches [27]. Since Si and Ge are elastically anisotropic, having a Zener ratio of 1.56 and 1.67, respectively, the stress and strain states will be dependent on the growth axis; however, the qualitative conclusions of the elasticity calculations will be similar.

It should be noted that others have also approached the problem of an epitaxial core–shell structure, but they have taken a slightly different approach [28,29]. The work by Gutkin et al. takes a similar approach but ignores strain in the axial direction of the nanowire. In the work by Liang et al., pressure vessel theory is used to calculate the strain state. The limitation of applying pressure vessel theory is that it again assumes the system is only stressed in the radial direction. In addition, both studies assume that the core and shell have identical elastic properties. While it is true that Si and Ge have similar elastic properties, this work takes the more rigorous approach, which is applicable to a broader set of materials.

3. Results and discussion

To explore the implications of this model, consider the case of a Ge shell grown on a Si nanowire substrate in comparison to a Ge film grown on a planar Si substrate for the similarly sized systems. The planar strain state is determined by an analogous approach to that used to determine the strain state of the nanowire and is

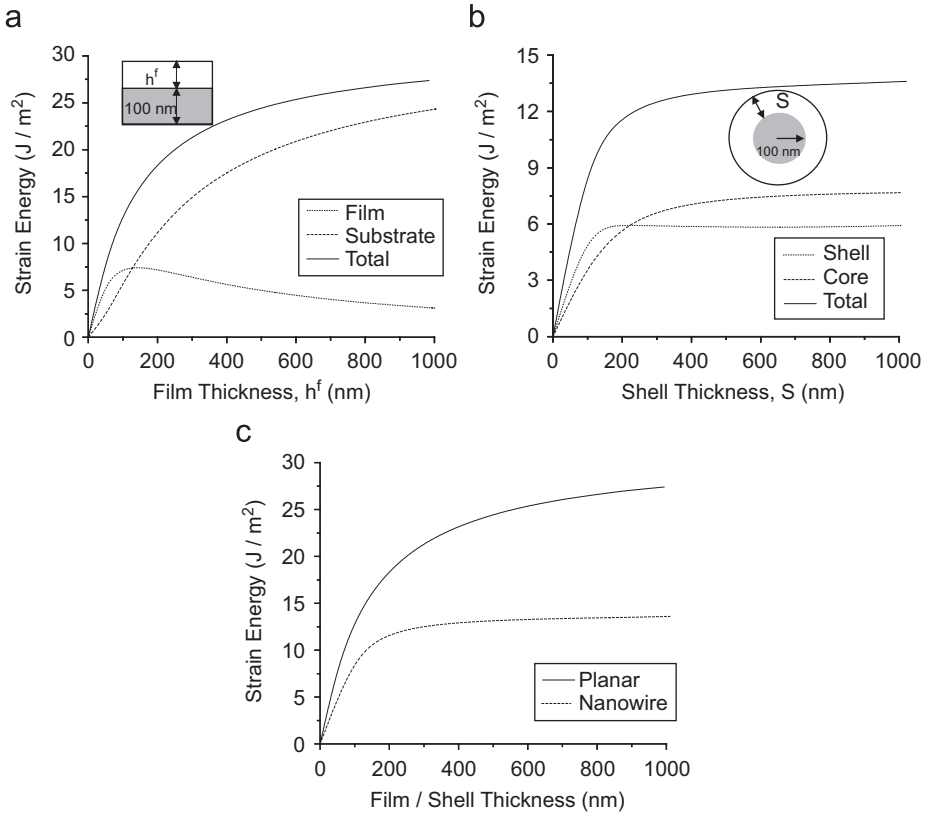

Fig. 3. Strain energy in system with a 100 nm Si core/substrate as a function of Ge shell/film thickness: (a) strain energy partitioning of a Ge film grown on a 100-nm-thick Si substrate; (b) strain energy partitioning of a Ge shell grown on a Si core of radius 100 nm and (c) comparison of total strain energy between systems.

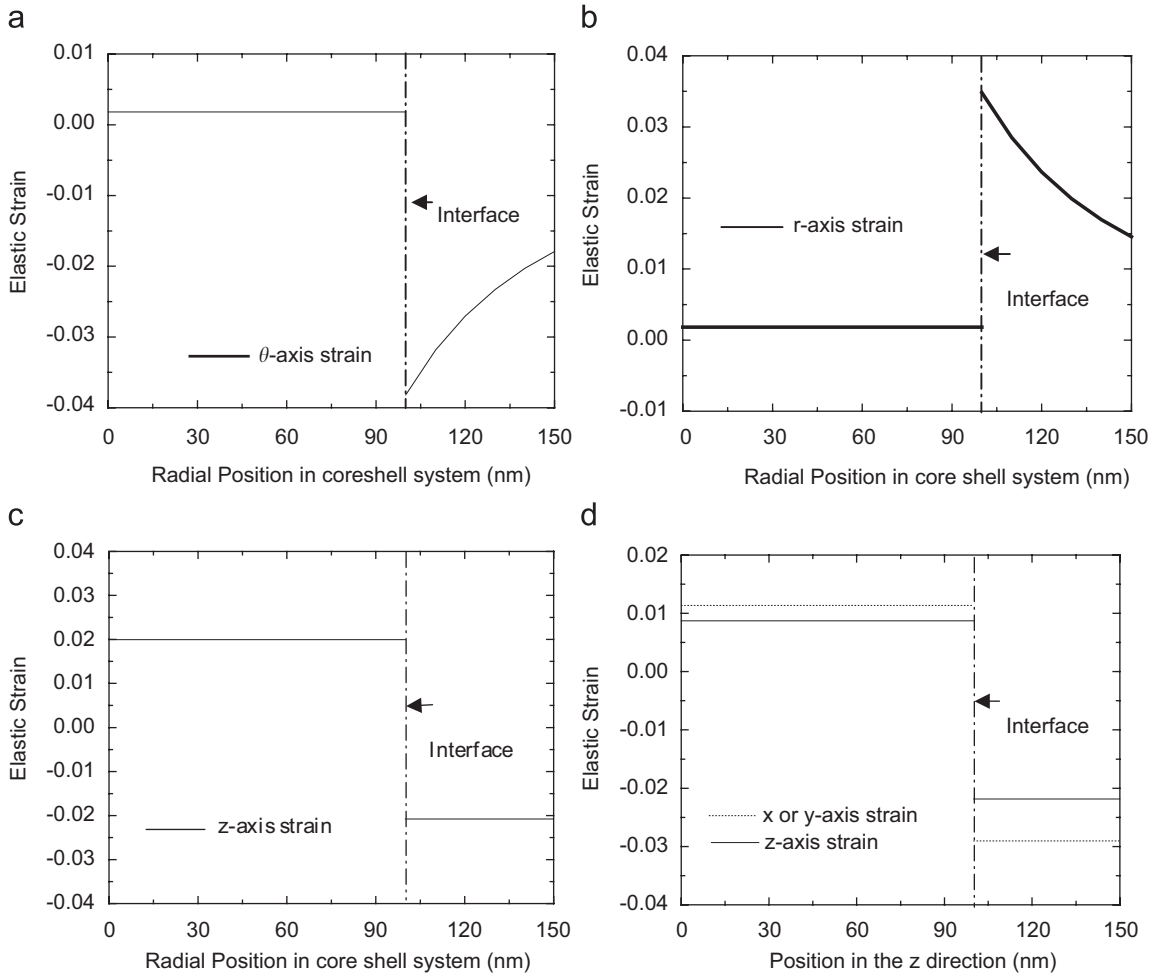

Fig. 4. (a) Elastic strain in the θ-direction as a function of the radial position, r, in the system with a core radius of 100 nm (core is Si) and shell thickness of 50 nm (shell is Ge); (b) elastic strain in the r-direction as a function of the radial position, r, in the system with a core radius of 100 nm (core is Si) and shell thickness of 50 nm (shell is Ge); (c) elastic strain in the z-direction as a function of the radial position, r, in the system with a core radius of 100 nm (core is Si) and shell thickness of 50 nm (shell is Ge); and (d) elastic strain in the x, y and z directions as a function of the position, z, in the system with a substrate thickness of 100 nm (substrate is Si) and the film thickness of 50 nm (film is Ge).

shown in Appendix 1. Throughout this discussion, the strain energy refers to the strain energy per interfacial area. The quantitative values presented here are specifically for $\langle 100 \rangle$ growth axis nanowires, but the trends and qualitative conclusions will be the same for any nanowire geometry.

In Fig. 3, we plot the calculated values of the strain energy in system with a 100 nm Si core/substrate as a function of Ge shell/film thickness. Fig. 3a depicts the strain energy partitioning of a Ge film grown on a Si substrate. For films much thinner than the substrate thickness, most of the strain energy is partitioned to the film and only a small amount is associated with the substrate. For relatively thick films, however, the roles of the film and substrate invert, and the strain energy in the film approaches zero. In core–shell system, qualitatively different behavior is observed. Fig. 3b shows that for Ge shell grown on a Si core of radius 100 nm, while for very thin shells the strain energy in the shell is much greater than that in the core, even for very thick shells the strain energy in the shell never converges to zero. The strain energy converges to a constant value much quicker in the nanowire geometry and remains partitioned between the two layers. Fig. 3c shows the comparison of the total strain energies between systems. It shows that as the ratio of the shell thickness to core radius approaches zero, the strain energy in the core–shell system converges to that in the planar system, as would be expected. It also shows that the total strain energy in the core–shell system is lower than that in the planar system with the same shell/film thickness. This allows for a larger critical thickness when growing a shell as opposed to those found in the planar case.

We can understand the qualitatively different behavior in the nanowire system in terms of the partial relaxation of the strain as a function of distance from the interface. In Fig. 4a–c, we plot the elastic strain as a function of radial position, r, in a core–shell nanowire. In this case, Si core thickness is 100 nm and Ge shell is 50 nm. Fig. 4a and b show the θ-axis strain and r-axis strain dependence of r. Fig. 4c shows the z-axis strain dependence of r. We can see that there is a large amount of strain in the core and shell at the interface since the lattice spacing at the interface must be matched as a condition for epitaxy. The r-axis strain and θ-axis strain are relaxed as the outside free surface of the shell is approached. However, the z-axis strain cannot be relieved at the outside surface. The z-axis strain is constant through the core and shell. This behavior is same as the similar-sized planar case, as shown in Fig. 4d. The ability to relax the θ-axis and r-axis strains away from the interface gives rise to pronouncedly lower strain energy in the nanowire geometry and potentially greater flexibility to design coherently strained structures.

Before we look at the exact limits of coherency, it is first important to consider how these shells might lose coherency with the underlying core. In the case of thin films grown on substrates, there exists a critical thickness at which the interfacial strain

energy becomes high enough that it is energetically favorable for misfit dislocations to form [7,8]. There are several ways to calculate this critical thickness, the most common being the so-called Matthews–Blakeslee (MB) criterion. According to this method, the critical thickness occurs once the energy of the system with a dislocation becomes lower than the energy due to coherency strain [28,29]. While other groups have attempted to apply this same logic to the current system [30,31], it is not certain that misfit dislocations are the dominant mechanism for loss of coherency of a shell around a core. In fact, some work has shown that instead of forming misfit dislocations at a certain thickness it may instead be energetically favorable to form islands (so-called Stranski–Krastanow growth) in Si–Ge core–shell nanowires [6]. This is similar to Stranski–Krastanow growth observed in the planar geometry [10,11]. For the purposes of the present work, we shall leave open the question of how the strain is relieved. It is assumed that there is some shell thickness at which the strain energy becomes high enough that coherent epitaxial growth is no longer energetically favorable. We will discuss the symmetry of the nanowire problem, how it compares to the planar case, and how we expect this symmetry to affect the critical thickness of the epitaxial core–shell nanowire.

In the planar case, the interface is very large in both the x and y directions as compared to the z-direction, and due to the cubic symmetry of the Si–Ge system the coherency strains will be isotropic within the plane of the film. In the core–shell system, however, the interface plane is the z–θ plane and the lower symmetry leads to anisotropy in the components of the elastic strain in the interface plane, and so we might expect anisotropic instabilities. Fig. 5 plots the elastic strain in the interface plane as a function of shell thickness when the core thickness is 100 nm. Fig. 5a shows in the core the elastic strains in the z and θ directions diverge, with the elastic strain in the z partitioned to the core more rapidly as a thicker shell is grown. Fig. 5b shows in the shell side the elastic strain in the θ-direction is larger than in the z-direction. All components of the elastic strain in the shell are a maximum for an infinitesimally thin shell and then decrease with shell thickness as the strain energy is gradually partitioned to the core.

Even though the exact strain relief mechanism is unclear, we can use the work done on the misfit dislocation formation in the planar case to study certain trends in the limits of epitaxy and see how they might play out in our model. The following is not a rigorous quantitative analysis, but rather an attempt to utilize approaches from planar studies in order to evaluate differences between the planar system and our core–shell model. In fact, any rigorous analysis would have to take into account the potential active slip systems, which will depend upon the nanowire growth axis.

We assume there is some critical energy in the system, f_{cr}, which if the system surpasses along any direction, misfit dislocations appear. Just as in work done on thin films, we define a critical shell thickness, S_{cr}, above which a shell cannot be grown when the core is rather large and all strain is in the shell. Similar to the work by Lo for planar films, however, our model predicts that as the core shrinks one can grow a thicker shell and still be below f_{cr} because the total strain energy is partitioned between layers [12,13]. The equations used by People and Bean [32] are used here to determine the critical energy. In their approach, People and Bean determine the critical thickness as the thickness at which the strain energy of a coherent system becomes larger than the energy associated with the dislocation of minimum energy, namely a screw dislocation [32]. While the critical energy used in the approach is a function of film thickness, we make the simplification that it is constant.

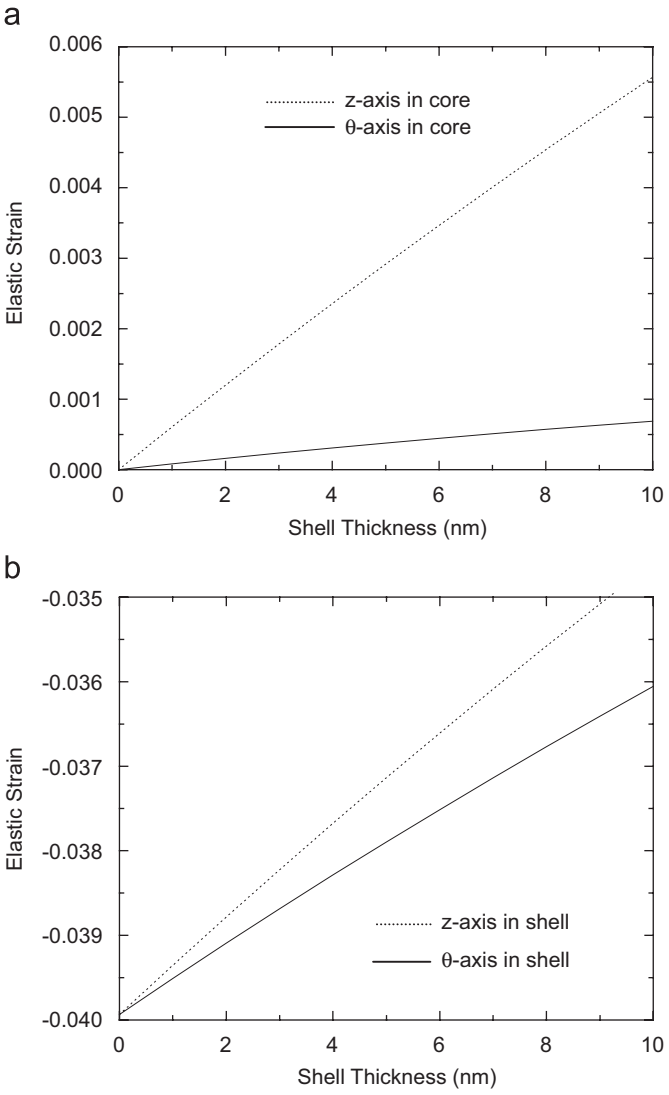

Fig. 5. Elastic strain in the interface plane as a function of shell (Ge) thickness in the system with a 100 nm core (Si) (a) elastic strain in the z- and θ-directions in the core side and (b) elastic strain in the z- and θ-directions in the shell side.

In the planar case, a system with film strain energy greater than f_{cr} is equally likely to form a dislocation in the x- as in the y-direction, but since the strains in the z-direction are generally higher (Fig. 2) the limits of epitaxy should be reached in the z-direction first. A stability map can be created such that stability corresponds to

$$(f_\theta^s + f_\theta^c) < f_{cr}$$
$$(f_z^s + f_z^c) < f_{cr}$$

Specifically, $f_{cr} = 0.307\,\mathrm{J/m^2}$ and $S_{cr} = 2.74\,\text{Å}$. Fig. 6 plots the theoretical shell thickness as a function of core radius below which misfit dislocations would not occur. Looking at this figure, strain energy in the core limits the coherency of the system when core radius is less than 10 nm. Since the strain is relieved in the θ-direction, epitaxial failure occurs preferentially in the z-direction over the θ-direction. In other words, if the strain relief in the θ-direction could be prevented, at a larger shell thickness the strain energy would become great enough in the z-direction to cause dislocation formation, and the shell might lose coherency with the underlying core. When core radius is more than 10 nm, however, strain energy in the shell limits the coherency of system. Epitaxial failure occurs preferentially in the θ-direction over the

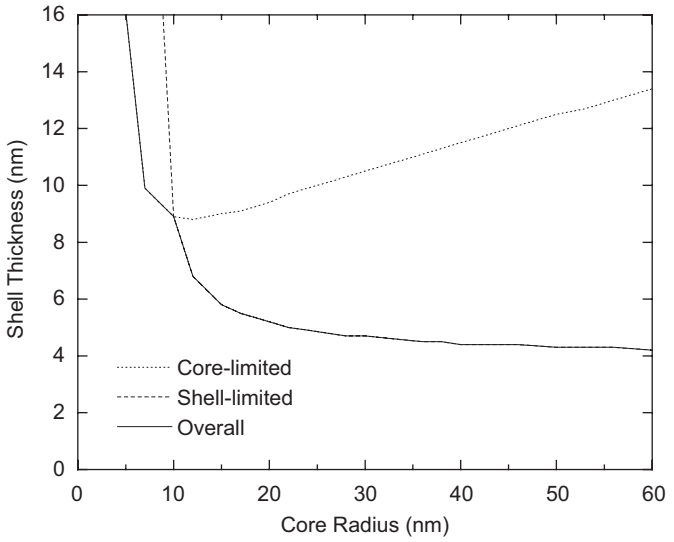

Fig. 6. The critical shell thickness as a function of core radius below which misfit dislocations would not occur.

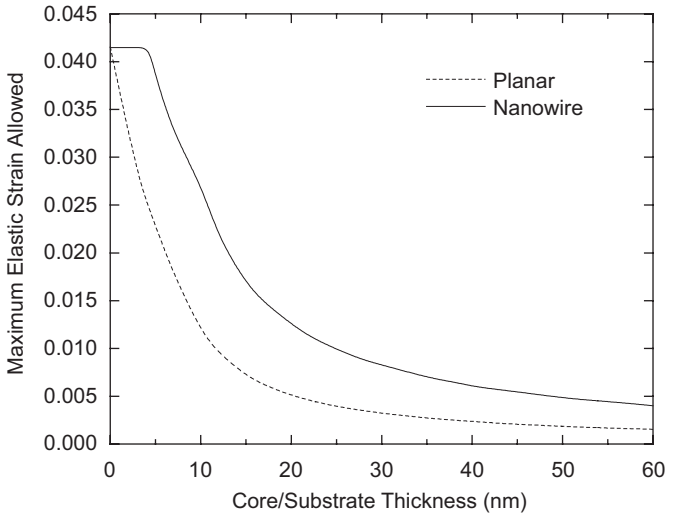

Fig. 7. For a given substrate size (thickness for planar and radius for core–shell), the hypothetical maximum strain in the substrate that could be accommodated in the *x*- or *y*-direction for planar, or *z*-direction for core–shell.

z-direction. At a thicker shell thickness the strain energy would become great enough in the θ-direction to cause dislocation formation. In reality, the nucleation of defects is a thermally activated process, so if shells can be grown at low temperatures it is possible to have a metastable system with critical thicknesses greater than predicted by theory [32].

As mentioned before, distinct advantages can be gained in the carrier mobility of Si and Ge if strain can be added to the materials in the direction of current transport [14–18]. While this can be either the *x*- or the *y*-direction in the planar system, we consider it to be the *z*-direction in the core–shell system. Fig. 7 shows the maximum achievable elastic strain in the direction of transport for both the planar and core–shell system as a function of substrate thickness. For the planar case it is assumed that the Si substrate is strained and in the core–shell system, it is assumed that the Si core is strained. Since the Si undergoes tensile strain, an increase in the electron mobility is expected [14,15]. As can be seen, for moderately thin structures a wire can accommodate more strain than the

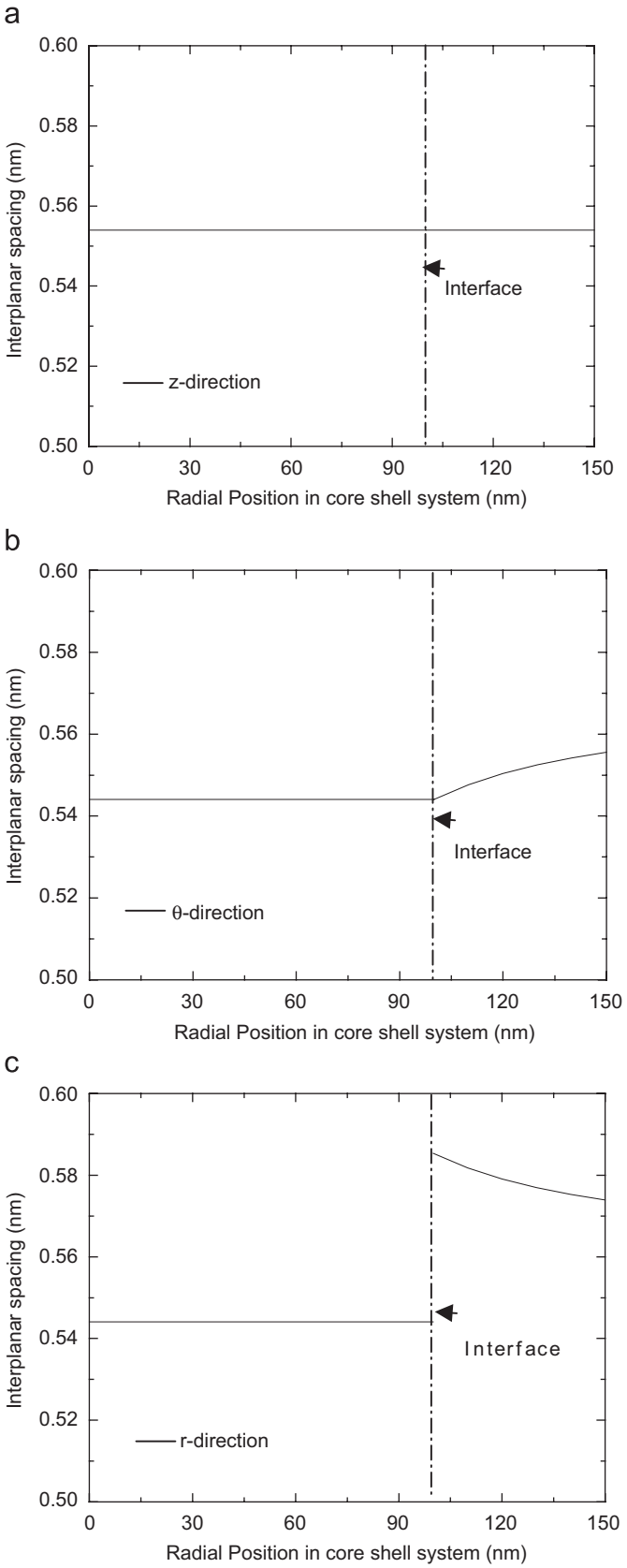

Fig. 8. (a) Interplanar spacing of planes in the *z*-direction as a function of radial position for a 50 nm shell grown on a core of radius 100 nm; (b) interplanar spacing of planes in the θ-direction as a function of radial position for a 50 nm shell grown on a core of radius 100 nm; and (c) interplanar spacing of planes in the *r*-direction as a function of radial position for a 50 nm shell grown on a core of radius 100 nm.

planar structure. For very thin cores with relatively thick shells, all of the strain is partitioned to the core and the maximum elastic strain is equal to the misfit between the core and shell. Eventually, a similar strain partitioning is seen in the planar case, but it occurs at smaller substrate sizes. As the figure shows, it is possible strain a nanowire more as compared to a planar structure of the same thickness if both are strained to the limit of epitaxy.

In addition to considering the strain energies and the effects on the limits of coherency, we can also consider the interplanar spacings of the system. Fig. 8 plots the interplanar spacing of planes in the r, θ and z directions as a function of position r. In this case, the shell thickness is 50 nm and core radius is 100 nm. Fig. 8a and b shows the interplanar spacings of the shell in the z and θ directions at the interface will match those of the underlying core. Fig. 8c shows the interplanar spacing of the shell in the r-direction at the interface will be slightly different from that of the underlying core. With this information in mind, we can predict the selected area electron diffraction pattern based on the results of our model. In the axial direction, the interplanar spacing is the same throughout the whole system, so a single diffraction spot for both the core and the shell should be observed. If the wire is grown and oriented in such a way as to have planes lying in the radial direction, these planes exhibit a constant interplanar spacing in the core, but a slightly varying interplanar spacing in the shell, as seen in Fig. 8c. Two spots are present in the radial direction, one corresponding to the core and the other corresponding to the shell. In fact, such a diffraction pattern has been shown by Lauhon et al. [3] in the case of a Ge shell grown around a Si core. While there is one interplanar spacing in the radial direction throughout the core, the interplanar spacing in the shell changes slightly, thus suggesting that there is a smeared spot in the diffraction pattern. In practice, this might be difficult to differentiate from the small volume effects [33].

4. Conclusions

In summary, we have developed a model to determine the strain state of an epitaxial core–shell nanowire structure and have used the example of a Ge shell grown on a Si core. In order to determine if such a structure provides any advantages over a standard planar heterostructure, we have examined several important issues. The first is the strain energy per interfacial area in each system, and it is shown that a core–shell nanowire has a lower energy than an analogous planar heterostructure. The second issue is the limit of epitaxy, based on a reasonable estimate of the critical energy to form misfit dislocations. Next, for the mobility enhancement strain provides, the maximum achievable strain in substrates of varying thicknesses is analyzed, again with the conclusion that nanowires offer greater flexibility. Finally, the behavior of the core–shell system is examined in the vicinity of the free surface of the shell. The conclusion reached is that the ability to relax the strain as this free surface is approached is the reason for all of these advantages over the planar system.

Acknowledgments

This work was supported by the National Science Foundation through Grants DMR-0304178 and ECS 06-09282.

Appendix 1. Strain state of planar heterostructure

This takes an analogous approach to that taken in the cylindrical case in order to set up the problem.

This heterostructure has the geometry of that shown in Fig. 1b. Due to the symmetry of the problem, we work in Cartesian coordinates with x, y, and z defining our system. The interface is in the x–y plane at $z = 0$, and is considered to be infinite in the x and y directions. We assume a film such that the thickness of the film is h^{f} and the unstrained lattice spacing is $a_{\mathrm{o}}^{\mathrm{f}}$. Similarly, we assume a substrate such that the thickness of the substrate is h^{s} and the unstrained lattice spacing is $a_{\mathrm{o}}^{\mathrm{s}}$. In the following symbols, a superscript denotes the relevant layer (f or s), and a subscript either denotes the relevant direction (x, y, z) or the fact that it is a constant in all directions (0).

The process of making an epitaxial heterostructure is divided into two steps. The first step is to adjust both layers to some reference state such that they both have the same lattice spacing, namely that of the reference, a_{o}^{r}. The choice of reference state is arbitrary and does not affect the final outcome. We adjust to the reference state in all directions, meaning each layer is being uniformly contracted or expanded. In each layer we can define the misfit to the reference as follows:

$$em_0^n = \frac{a_0^n - a_0^r}{a_0^r} \tag{A.1}$$

As a result of the first step, the system is epitaxial. Even though it may be epitaxial, the system is not at its ideal configuration as it has been artificially put in this configuration without regard to balancing stresses on the system. In the next step, the system is allowed to relax. In general, this relaxation can be different in different directions. This relaxation corresponds to the displacement, $u_i{}^n$, of each layer. In order for the system to remain epitaxial, the displacement must be continuous at the interface. In mathematical terms, at $z = 0$:

$$u_i^{\mathrm{f}} = u_i^{\mathrm{s}} \tag{A.2}$$

After displacement, at each point in each layer the system can be characterized by the strained lattice spacings a_i^n. Note that the final lattice spacing can in general be different in each layer and in each direction. We can define the displacement strain $\varepsilon_i{}^n$ as the strain between the final state and the reference state:

$$\varepsilon_i^{\mathrm{f}} = \frac{a_i^n - a_0^r}{a_0^r} \tag{A.3}$$

As a result of this misfit correction followed by relaxation process, there is an induced elastic strain e_i^n in each layer. This elastic strain arises from the misfit strain in Eq. (A.1) and from the displacement strain in Eq. (A.3) such that it is expressed as

$$e_i^n = \frac{a_{\mathrm{o}}^r}{a_{\mathrm{o}}^n}\left(u_i^n - em_{\mathrm{o}}^n\right) \tag{A.4}$$

The negative sign is due to the sign convention used to define the misfit strain, and $a_{\mathrm{o}}^r/a_{\mathrm{o}}^n$ is a correction factor so that the elastic strain in a layer is in reference to that layer and not the reference state.

The strain state of the heterostructure has been described in its most general form. Now we use some basic premises of elasticity theory to determine some relevant relationships [19]. First of all, the displacement relates to the displacement strain as follows:

$$\varepsilon_{ij}^n = \frac{1}{2}\left(\frac{\partial u_i^n}{\partial j} + \frac{\partial u_j^n}{\partial i}\right) \tag{A.5}$$

For this case we assume only normal strains. This implies that u_i^n is a function of only i and that Eq. (A.5) can be simplified to

$$\varepsilon_{ij}^n = \frac{\partial u_i^n}{\partial i} = \varepsilon_i^n \tag{A.6}$$

Now the elastic strain is in terms of the unstrained lattice spacings, the reference lattice spacing, and the displacement

functions. We can determine the stresses $\sigma_i{}^n$ in the system if we use the simplified stiffness matrix for cubic symmetry to obtain the following:

$$\sigma_x^n = C_{11}^n e_x^n + C_{12}^n e_y^n + C_{12}^n e_z^n \tag{A.6a}$$

$$\sigma_y^n = C_{12}^n e_x^n + C_{11}^n e_y^n + C_{12}^n e_z^n \tag{A.6b}$$

$$\sigma_z^n = C_{12}^n e_x^n + C_{12}^n e_y^n + C_{12}^n e_z^n \tag{A.6c}$$

$$\tau_{xy}^n = \tau_{xz}^n = \tau_{yz}^n = 0 \tag{A.6d}$$

In order to satisfy the condition that the force acting on an element of the system be zero, we impose the stress equilibrium conditions:

$$\frac{\partial(\sigma_x^n)}{\partial x} + \frac{\partial(\tau_{xy}^n)}{\partial y} + \frac{\partial(\tau_{xz}^n)}{\partial z} = 0 \tag{A.7a}$$

$$\frac{\partial(\sigma_y^n)}{\partial y} + \frac{\partial(\tau_{xy}^n)}{\partial x} + \frac{\partial(\tau_{yz}^n)}{\partial z} = 0 \tag{A.7b}$$

$$\frac{\partial(\sigma_z^n)}{\partial z} + \frac{\partial(\tau_{yz}^n)}{\partial y} + \frac{\partial(\tau_{xz}^n)}{\partial x} = 0 \tag{A.7c}$$

Inserting (A.6a–A.6c) into (A.7a–A.7c) and neglecting shear stresses, we determine

$$\frac{\partial^2(u_i^n)}{\partial i^2} = 0 \tag{A.8}$$

Therefore u_i^n and ε_i^n take the form

$$u_i^n = L_i^n i + M_i^n \tag{A.9}$$

$$\varepsilon_i^n = L_i^n \tag{A.10}$$

We are only concerned with the strain state, and so we can neglect the M_i^n terms in (A.9). Furthermore, since the system has cubic symmetry and the system is essentially infinite in both x and y directions, we assume the strain state in the x-direction to be equivalent to the strain state in the y-direction. In other words:

$$L_x^n = L_y^n \tag{A.11}$$

Therefore, the displacements, displacement strains, elastic strains, and stresses are equivalent in the x- and y-directions.

Now we describe the strain state in terms of the four remaining integrations constants, the unstrained lattice spacings, the reference state, and the elastic properties of the film and substrate. We can look at some of the constraints on the system in order to determine the unique solution.

1. The displacement in the x-direction should be continuous at the interface:

$$u_x^f|_{z=0} = u_x^s|_{z=0} \tag{A.12}$$

This equation guarantees epitaxy in the x-direction.

2. The displacement in the y-direction should be continuous at the interface:

$$u_y^f|_{z=0} = u_y^s|_{z=0} \tag{A.13}$$

This equation guarantees epitaxy in the y-direction. It is redundant after Eq. (A.12) as we have already said L_x^n and L_y^n are equivalent.

3. The displacement in the z-direction should be continuous at the interface:

$$u_z^f|_{z=0} = u_z^s|_{z=0} \tag{A.14}$$

This equation simplifies to $0 = 0$, so Eq. (A.14) is always satisfied.

4. Assume a plane stress situation such that the stresses normal to the interface are zero:

$$\sigma_z^f = \sigma_z^s = 0 \tag{A.15}$$

5. The net forces on the free surfaces must be zero. The net force on the two (0 0 1) surfaces is zero as a result of Eq. (A.15). The net forces on the (1 0 0) and (0 1 0) surfaces are equivalent and each must balance according to

$$\sigma_x^f hf + \sigma_x^s hs = 0 \tag{A.16}$$

One unknown can be eliminated in each of the Eqs. (A.12), (A.16), and Eq. (A.15) can be used to eliminate two unknowns. After this process of elimination, we are left with a description of the strain state of the system in terms of the elastic constants, the unstrained lattice spacings, the reference state lattice spacing, and the relative thicknesses of the two layers.

In order to determine the elastic strain energy per interfacial area f^nin each layer, we can use the equation

$$u^n = \tfrac{1}{2}(\sigma_x^n e_x^n + \sigma_y^n e_y^n)h^f \tag{A.17}$$

Note that there is no term due to the stress in the z-directions since it was set to zero in (A.15). Since the x- and y-direction play equal roles in this model, it can be assumed that the contributions to the strain energy from strains in the x- and y-directions are equal.

References

[1] S.M. Sze, Physics of Semiconductor Devices, Wiley, New York, 1969.
[2] Y.Y. Wu, R. Fan, P.D. Yang, Nano Lett. 2 (2002) 83.
[3] M.S. Gudiksen, L.J. Lauhon, J. Wang, D.C. Smith, C.M. Lieber, Nature 415 (2002) 617.
[4] L.J. Lauhon, M.S. Gudiksen, C.M. Lieber, Math. Phys. Eng. Sci. 362 (2004) 1247.
[5] Y.W. Heo, C. Abernathy, K. Pruessner, W. Sigmund, D.P. Norton, J. Appl. Phys. 96 (2004) 3424.
[6] L. Pan, K.-K. Lew, J.M. Redwing, E.C. Dickey, Nano Lett. 5 (2005) 1081.
[7] S. Lee, S.D. Wang, C.H. Hsueh, Mater. Sci. Eng. A309 (2001) 473.
[8] A. Subramaniam, J. Appl. Phys. 95 (2004) 8472.
[9] C.H. Hsueh, J. Crystal Growth 258 (2003) 302.
[10] Y.-W. Mo, D.E. Savage, B.S. Swartzentruber, M.G. Lagally, Phys. Rev. Lett. 65 (1990) 1020.
[11] D.J. Eaglesham, M. Cerullo, Phys. Rev. Lett. 64 (1990) 1943.
[12] P. Wakeland, T. Khraishi, D. Zubia, J. Electron. Mater. 32 (2003) 836.
[13] Y.H. Lo, Appl. Phys. Lett. 59 (1991) 2311.
[14] S.F. Nelson, K. Ismail, J.O. Chu, B.S. Meyerson, Appl. Phys. Lett. 63 (1993) 367.
[15] J. Welser, J.L. Hoyt, J.F. Gibbons, IEEE Electron Device Lett. 15 (1994) 100.
[16] R.J.H. Morris, D.R. Leadley, R. Hammond, T.J. Grasby, T.E. Whall, E.H.C. Parker, J. Appl. Phys. 96 (2004) 6470.
[17] D.R. Leadley, M.J. Kearney, A.I. Horrell, H. Fischer, L. Risch, E.H.C. Parker, T.E. Whall, Semicond. Sci. Technol. 17 (2002) 708.
[18] C.M. Warwick, T.W. Clyne, J. Mater. Sci. 26 (1991) 3817.
[19] S.P. Timoshenko, J.N. Goodier, Theory of Elasticity, McGraw-Hill Book, New York, 1970, p. 400.
[20] H.F. Wolf, Silicon Semiconductor Data, Pergamon Press, Oxford, 1969.
[21] F. Schaffler, Properties of Advanced Semiconductor Materials GaN, AlN, InN, BN, SiC, SiGe, Wiley, New York, 2001, p. 149.
[22] K.-K. Lew, L. Pan, E.C. Dickey, J.M. Redwing, Adv. Mater. 15 (2003) 2073.
[23] X. Zhang, J. Kulik, E.C. Dickey, J. Nanosci. Nanotechnol. 7 (2007) 717.
[24] T.I. Kamins, X. Li, R. Stanley, Williams, Nano Lett. 4 (2004) 503.
[25] S. Ge, K. Jiang, X. Lu, Y. Chen, R. Wang, S. Fan, Adv. Mater. 17 (2005) 56.
[26] H. Jagannathan, M. Deal, Y. Nishi, J. Woodruff, C. Chidsey, P.C. Mclntyre, J. Appl. Phys. 100 (2006) 024318.
[27] D. Zschech, D.H. Kim, A.P. Milenin, R. Scholz, R. Hillebrand, C.J. Hawker, T.P. Russell, M. Steinhart, U. Gösele, Nano Lett. 7 (2007) 1516.
[28] M.Y. Gutkin, I.A. Ovid'ko, A.G. Sheinerman, J. Phys.: Condens. Matter 2000 (2000) 5391.
[29] Y. Liang, W.D. Nix, P.B. Griffin, J.D. Plummer, J. Appl. Phys. 97 (20) (2005) 043519.
[30] S.C. Jain, M. Willander, Silicon-Germanium—Strained Layers and Heterostructures, Academic Press, Amsterdam, 2003, p. 74.
[31] I. Matthews, A.E. Blakeslee, J. Crystal Growth 27 (1974) 118.
[32] R. People, J.C. Bean, Appl. Phys. Lett. 47 (1985) 322.
[33] D.B. Williams, C.B. Carter, Transmission Electron Microscopy, Plenum Publishing, New York, 1996, p. 255.